ARTICLE

JAAS www.rsc.org/jaas

Precise analysis of the $^{228}Ra/^{226}Ra$ isotope ratio for short-lived U-series disequilibria in natural samples by total evaporation thermal ionization mass spectrometry (TE-TIMS)

Tetsuya Yokoyama* and Eizo Nakamura

The Pheasant Memorial Laboratory for Geochemistry and Cosmochemistry, Institute for Study of the Earth's Interior, Okayama University at Misasa, Tottori-ken, 682-0193 Japan. E-mail: yokoyama@misasa.okayama-u.ac.jp; eizonak@misasa.okayama-u.ac.jp; Fax: +81-858-43-2184; Tel: +81-858-43-1215

Received 19th January 2004, Accepted 10th March 2004
First published as an Advance Article on the web 17th May 2004

We report a new analytical technique for precise and accurate determination of the $^{228}Ra/^{226}Ra$ ratio by total evaporation thermal ionization mass spectrometry (TE-TIMS). An improved chromatographic separation method employing a new tandem column technique that enables high yield and high purity of Ra is also described. Repeated analysis of Ra standard solution ($^{228}Ra/^{226}Ra = 1.1$) yielded an analytical reproducibility for $^{228}Ra/^{226}Ra$ ranging from 0.2% to 0.9% (2σ) for 170 to 2 fg of Ra. Reproducibility was strongly controlled by counting statistics of $^{226}Ra^+$ and $^{228}Ra^+$ ion beam intensities collected by an ion counting detector, implying that in-run precision for Ra isotope analysis of our method can be evaluated using a counting statistics law. Determination of ^{226}Ra abundances in silicate rock samples were examined by isotope dilution TE-TIMS, and reproducibility was 0.3% (2σ) for JR-2 ($^{226}Ra = 3700$ fg g^{-1}) and 0.6% (2σ) for JB-2 ($^{226}Ra = 81$ fg g^{-1}); the reproducibility of these measurements are 2–3 times better than previously published conventional TIMS procedures. The $^{226}Ra/^{228}Ra$ ratio in natural samples can be also measured with an analytical uncertainty of $\sim$1% (2σ). The accuracy of our method was confirmed by measuring ($^{226}Ra/^{230}Th$) and ($^{228}Ra/^{232}Th$) ratios for JR-2, a sample old enough (1 Ma) to be in ^{230}Th–^{226}Ra and ^{232}Th–^{228}Ra radioactive equilibria. Our method is especially effective for samples with a very low abundance of Ra.

1. Introduction

Uranium-series disequilibria of short-lived nuclides in geological materials are important tracers to understand the timescales of various Quaternary-aged geological processes. Radium in natural samples usually has two radioactive isotopes (^{226}Ra: $T_{1/2} = 1600$ yr; ^{228}Ra: $T_{1/2} = 5.75$ yr), which are daughter nuclides of ^{230}Th ($T_{1/2} = 7.57 \times 10^4$ yr) and ^{232}Th ($T_{1/2} = 1.40 \times 10^{10}$ yr). The systematics of ^{230}Th–^{226}Ra and ^{232}Th-^{228}Ra disequilibria can, theoretically, reveal geological processes occurring on timescales ranging from 8000 yr to 100 yr and from 30 yr to <1 yr, respectively, and have been applied to various geological fields such as volcanology and hydrology as useful chronological tools.[1,2]

Improvements in mass spectrometry in the last 15 years have enabled precise determination of U–Th–Ra disequilibria as a substitute for conventional alpha and gamma counting methods. In particular, the recent instrumental and technical innovation of multi-collector inductively coupled plasma mass spectrometry (MC-ICP-MS) has demonstrated the potential for precise determination for U–Th–Ra disequilibria in natural samples better than that achieved *via* thermal ionization mass spectrometry (TIMS). This reflects the higher sensitivity attainable with plasma source ionization than with thermal ionization, and some dramatic improvements have been reported, especially for thorium, which is difficult to effectively ionize by TIMS due to the high first ionization potential of thorium (6.08 eV).[3,4] However, radium has a relatively low first ionization potential (5.28 eV) and, for radium, TIMS has a detection sensitivity >20 times higher than MC-ICP-MS[4] (hereafter "detection sensitivity" implies the yield of ions available for measurement by a detector; the combination of ionization–transmission–detection efficiency). Furthermore, analytical disadvantages of ICP-MS (*e.g.*, larger instrumental mass fractionation, memory effects that cannot be neglected, and larger isobaric interferences due to hydrocarbons and/or hydrides) suggest that analysis by TIMS is likely to produce more favorable results. These facts pose serious challenges to precise and accurate determination of Ra when the amount of Ra used for single analysis becomes as small as a few femtogram levels (*e.g.*, the determination of ^{226}Ra for minerals in volcanic rocks). Therefore, it is advantageous to analyze Ra by TIMS rather than MC-ICP-MS in order to achieve the highly precise data required for geochemical discussions based on U–Th–Ra disequilibria.

Some authors have concluded that Ra mass fractionation during TIMS measurement was small enough to be neglected.[5,6] However, Pietruszka *et al.*[7] observed fractionation of $\sim$2%/amu from the start to the end of a $\sim$2.5 h analysis by TIMS. We observed a similar fractionation in our preliminary experiments, and found the fractionation difficult to suppress. Correction of mass fractionation during measurement is always problematic when the element does not have an isotope ratio of two non-radiogenic isotopes or artificially added isotopes for normalization. One of the most effective ways to precisely determine the isotope ratio without the correction of mass fractionation is a total evaporation TIMS (TE-TIMS) technique. For instance, Fiedler *et al.*[8] reported that the standard deviation of repeated $^{240}Pu/^{239}Pu$ ratio analyses decreased from 0.038% to 0.0077% when TE-TIMS was applied. However, at present there is no methodology in which Ra isotope analysis by TE-TIMS has been adopted.

Also important for the precise measurement of Ra isotopes in natural samples, for either TIMS or ICP-MS, is to obtain Ra at high purity to avoid potential analytical problems during mass spectrometry, such as isobaric mass interferences, matrix effects due to instrumental mass fractionation for MC-ICP-MS,[4] or decreased ionization efficiency for TIMS.[6,9] Because of the similar chemical characteristics of Ba and Ra in conventional cation-exchange resins, separation of Ra from Ba was

DOI: 10.1039/b400829d

difficult unless special separation techniques were employed (*e.g.*, the use of columns with small aspect ratio and EDTA as the eluant with severe pH adjustment).[5,6] By the development of a new extraction chromatographic resin supporting a crown ether (Sr resin, Eichrom),[10] the separation of Ra from Ba was easily achieved using an HNO_3 medium.[9] However, in our preliminary experiments, Ra ion beam intensities for natural samples separated by Chabaux's method were 2–3 times worse compared to the same size of pure Ra standard. Therefore, we modified the separation technique of Chabaux to improve the purification of Ra.

In this study, we report the first trial of Ra isotope analysis by TE-TIMS, together with an improved chromatographic separation method for Ra that enables high yield and high purity. Through the combination of these new techniques, we have established a method for precise and accurate determination of ^{226}Ra content and the $^{226}Ra/^{228}Ra$ ratio in natural samples, which is better than previous studies, by employing only a few femtograms of ^{226}Ra and ^{228}Ra. Half-lives of U, Th and Ra nuclides used for calculations in this study are taken from the internet web site of the Nuclear Wallet Card (6th edition, January 2000) supplied by Brookhaven National Laboratory, New York (http://www.nndc.bnl.gov/). Isotope ratios in parentheses represent activity ratios throughout this paper unless noted otherwise.

2. Experimental

All experiments in this study were carried out under clean conditions of class 100 at the Pheasant Memorial Laboratory (PML).[11]

2.1. Apparatus

Elution profiles of ion-exchange column chromatography for Mg, Ca, and 23 trace elements (Rb, Sr, Y, Zr, Cs, Ba, REEs, Pb, Th and U) were determined by a quadrupole-type ICP-MS (PMS2000, Yokogawa Analytical Systems), and those for Ra were determined by a high resolution sector type ICP-MS (Element, Finnigan). Detail of the quadrupole-pole type and the sector type ICP-MS are described in Makishima and Nakamura[12] and Makishima *et al.*,[13] respectively. Analytical errors for ICP-MS analyses were 5–10% for the quadrupole and $<5\%$ for the sector type.

Isotope analysis of Ra was carried out by a Finnigan MAT 262 TIMS ("INU"). Detail of this TIMS is described in Yokoyama *et al.*[14] Recovery yields and total blanks for chemical procedures were also determined by TIMS.

2.2. Reagents

Water and hydrochloric, nitric, and hydrofluoric acids were purified as described in Yokoyama *et al.*[15] Highly purified 70% perchloric acid (Tamapure-AA-100, Tama Chemical Co. Ltd.) and 85% phosphoric acid (Merck, Cat. No. 100552) were used without further purification.

To examine the elution profiles of some ion-exchange resins, a new multi-element standard solution (MES solution) containing 23 trace elements (Rb, Sr, Y, Cs, Ba, REE, Pb, Th, U, and Ra) was prepared in this study by adding Ra standard solution (NIST SRM4966) to the previous MES solution that was used in Makishima and Nakamura.[12] The mixture was dried and conditioned with 3 M HNO_3, and has a concentration of 10 pg mL^{-1} for Ra and 20000 PM (defined in Makishima and Nakamura[12]) for the rest of the elements.

Ta oxide was used as an ionization activator, and was prepared as follows: 0.1 g of pure Ta ribbon (Nilaco Co.) was washed with *aqua regia*, and dissolved in a mixture of 0.2 mL of 16 M HNO_3, 1 mL of 30 M HF, and 2 mL of water, with ultrasonic agitation overnight. Then, 0.06 mL of 85% H_3PO_4 and 1.8 mL of water were added. The solution was diluted ten-fold with water, resulting in 2 μg Ta per μL of solution.

2.3. Sample decomposition

Powdered rock samples (<0.5 g) were weighed and mixed with a ^{228}Ra enriched spike, and decomposed with HF–$HClO_4$ in Teflon beakers following the method of Yokoyama *et al.*[16] The decomposed solution was dried and dissolved by 1 M HCl. The amount of solution was in proportion to the sample size, which was 1 mL for <0.1 g of the sample, and $10W$ mL for W g ($W > 0.1$) of the sample. It was then centrifuged to separate the white precipitate of Ti-oxides, which was regarded as evidence of the suppression of insoluble fluorides.[16]

2.4. Separation of Ra

2.4.1. Preliminary removal of major elements. Our overall separation procedure is schematically shown in Fig. 1. Prior to the final purification, co-existing major cations in the sample solution (*e.g.* Mg^{2+}, Ca^{2+}, Al^{3+}, and Fe^{3+}) should be removed. In previous studies, this process was carried out by cation-exchange column chromatography with relatively large resin beds (>20 mL).[4,9] In this study, however, we used a very small (1 mL) cation-exchange column to reduce the Ra blank derived from the resin itself, and to avoid waste of resin and reagents. To enhance the distribution coefficient of Ra, a 1 : 1 mixture of AG50WX8 and AG50WX12 resins (200–400 mesh, Biorad) was used. Hereafter, the resin is referred to as the "mixed-resin".

Step 1. The "mixed-resin" was pre-washed as described in Yoshikawa and Nakamura,[17] and charged into a 1.0 mL polypropylene column (48 mm resin bed length). The resin bed was cleaned successively with 6 M HCl, water, 4 M HNO_3, and more water, and it was conditioned with 1 mL of 1 M HCl. In the case of smaller sample sizes (<0.1 g), step 2 (below) was omitted.

Step 2. For larger sample sizes only (>0.1 g), the sample solution, 3 mL maximum at a time, was loaded onto the column. The resin bed was washed with 4 mL of 2.8 M HCl to roughly remove major elements, and 3 mL of 4 M HNO_3 was subsequently added to the column to collect Ra. The resin bed was cleaned with 2 mL of water and again conditioned by 1 mL of 1 M HCl. This routine was repeated until all of the sample solution was passed through the column (see Fig. 1). When all of the sample solution had passed through, the resin bed was cleaned using 6 M HCl and water, and conditioned with 1 mL of 1 M HCl so that it could be re-used in the next step. The Ra fraction was dried and conditioned with 1 mL of 1 M HCl for the next step.

Step 3. The fraction containing Ra was loaded on to the column. The resin bed was then washed with 8 mL of 5 M HCl, and Ra was collected by subsequent addition of 3 mL of 4 M HNO_3. The Ra fraction was dried and conditioned with 0.3 mL of 3 M HNO_3, and this solution was introduced to the final purification process described in the next section.

2.4.2. Purification of Ra by tandem-column separation. The final purification of Ra was performed by two steps with two extraction chromatographic resins (Sr resin and TRU resin: Eichrom) and CG-71C (Amberchrom).

Step 4. Sr resin (100–150 μm particle) and TRU resin (100–150 μm particle) were separately charged into 0.5 mL polyethylene columns (43 mm resin bed length), which were cleaned successively with 1.5 M HF, 3 M HNO_3 and 0.1 M HNO_3. The

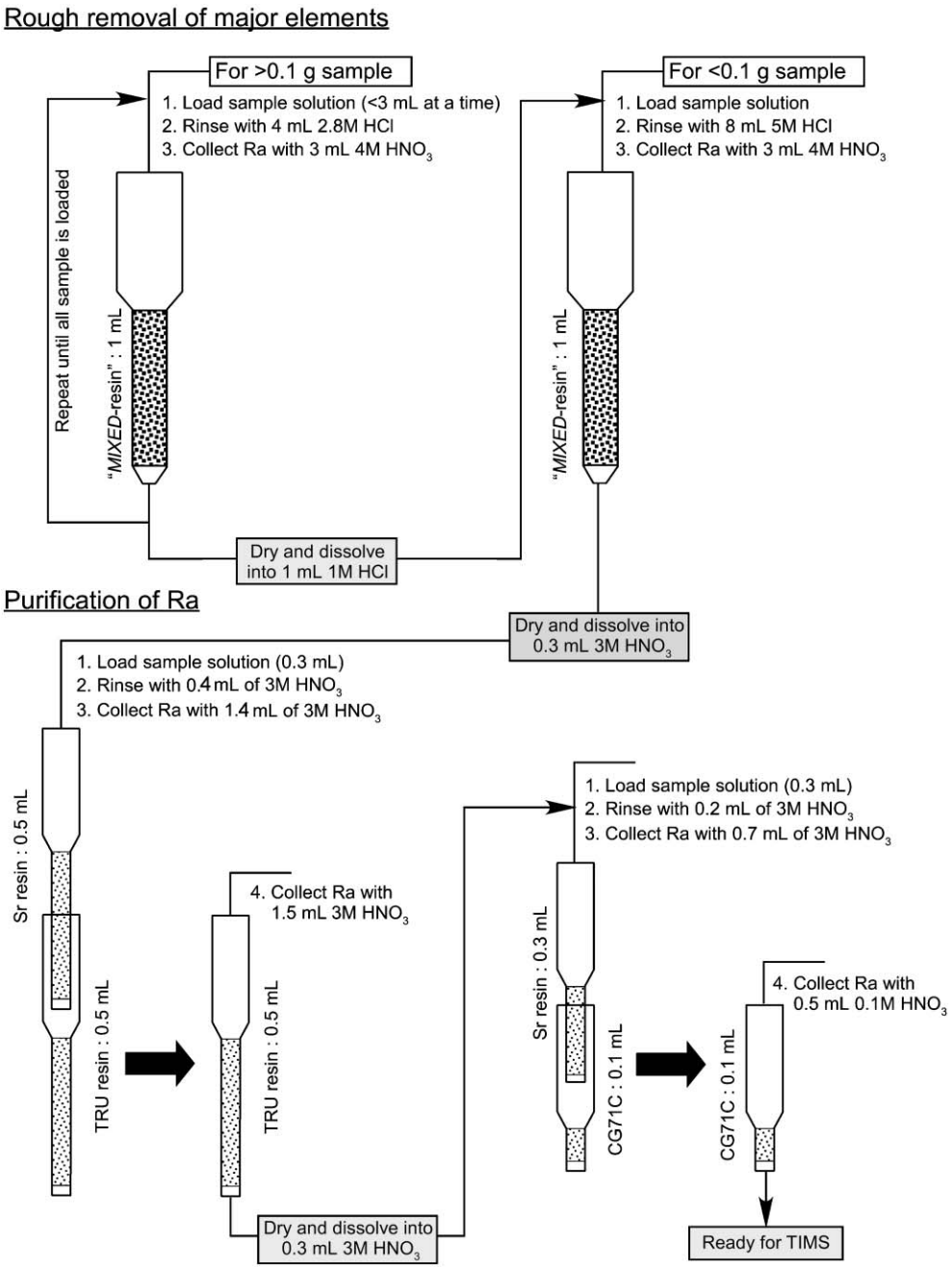

Fig. 1 Complete separation procedures of Ra from natural samples.

resin beds were conditioned by use of 1 mL of 3 M HNO_3. The sample solution (0.3 mL) was loaded on the Sr resin, and washed by 0.4 mL of 3 M HNO_3. The Sr resin column was then set vertically on the TRU resin (Fig. 1), and a Teflon beaker was placed under the TRU resin to collect Ra. 1.4 mL of 3 M HNO_3 was eluted from the top column. The top column was then removed, and 1.5 mL of 3 M HNO_3 was eluted from the TRU resin. This fraction was dried and conditioned with 0.3 mL of 3 M HNO_3.

Step 5. Sr resin and CG71C (120 μm particle) were charged into 0.3 mL and 0.1 mL polyethylene columns (26 mm and 9 mm resin bed lengths), respectively, and cleaned as described in Step 4. The sample solution (0.3 mL) was loaded on the Sr resin, and washed by 0.2 mL of 3 M HNO_3. Then the Sr resin column was set vertically on the CG71C (Fig. 1). Ra was collected by eluting 0.7 mL of 3 M HNO_3 from the top column, and eluting 0.5 mL of 0.1 M HNO_3 from the CG71C after removing the Sr resin. Before TIMS analysis, the Ra fraction was dried and repeatedly treated by the mixture of HNO_3, HF and $HClO_4$ in order to remove any organic matter remaining in this fraction.

2.5. Isotope analysis by total evaporation TIMS

Extracted Ra was loaded with 1 μL of Ta-oxide activator solution onto the top of trapezoid-shaped W filament (Nilaco) that was previously degassed at 5.4 A under a vacuum condition of $<10^{-3}$ Pa. To enhance ionization efficiency, Ra was loaded onto as small an area as possible on the filament (about 1 mm × 1 mm square). Prior to Ra isotope analyses, the baseline noise of the detector (a secondary electron multiplier: SEM) was analyzed once every 5 samples (see section 3.7.2), which was determined as a grand mean of 110 baseline scans (16 s integration per scan). The filament current was increased to reach the filament temperature of 900 °C over the course of 10 min, and then the filament was slowly increased to 1220–1250 °C. Ra isotope measurement was started when the initial

Ra^+ ion signal (10–100 cps, depending on the amount of Ra used) was detected by the SEM. A single scan of data collection consisted of two mass jumps at $m/z = 226$ and $m/z = 228$, and data were acquired for 4 s at individual masses for spiked runs ($^{228}Ra/^{226}Ra = 0.5$–5), and 4 and 8 s for $m/z = 226$ and 228 for non-spiked runs ($^{228}Ra/^{226}Ra < 0.01$). One block of data acquisition was comprised of 11 scans, and the filament current was increased at the end of each block. The filament current was incrementally increased by 50 mA for block #1–#3, 30 mA for #4–#10, 50 mA for #11–#15, 60 mA for #15–#20, and 70 mA for #21 and over. Data acquisition ended when Ra^+ ion signal intensity decreased to 5% of that for the most intense signal observed, typically at block #10–#15 irrespective of the amount of Ra used. The $^{228}Ra/^{226}Ra$ ratio was finally determined from the total ion currents of $^{226}Ra^+$ and $^{228}Ra^+$ ions that were integrated after raw-data smoothing by the modified Savitzky–Golay method[18] and time-drift correction of both signal acquisitions (Fig. 2). The total analytical time was approximately 60–90 min for one sample including initial filament heating time before data acquisition.

3. Results and discussion

3.1. Performance of our separation method

Fig. 3 shows elution profiles for the rough removal of major elements with the "mixed-resin" that are described in section 2.4.1. Ra is considered to possess a nearly identical partition coefficient, as does Ba for this resin in HCl and HNO_3 media unless special separation techniques are employed.[5,6] Therefore, the behavior of Ra on the "mixed-resin" is monitored by Ba as a proxy of Ra. Fig. 3a is the result of initial separation process for larger sample cases (step 2 of section 2.4.1), in which 0.3 g of natural sample (tholeiitic basalt from Miyakejima volcano, Japan: $SiO_2 = 51\%$) was used. As is shown in this figure, all Mg and >90% of Ca could be separated from Ra, while some proportion of REE and Sr (not shown) remained in the Ra fraction. Fig. 3b is the elution profiles of step 3 in which 0.1 g of basalt (Miyakejima) was examined. Although Mg, Ca, and Sr (not shown) were thoroughly separated from Ra, light–middle REE (La–Tb) could not be separated from Ra due to similar partition coefficients to the "mixed-resin" with respect to these elements.

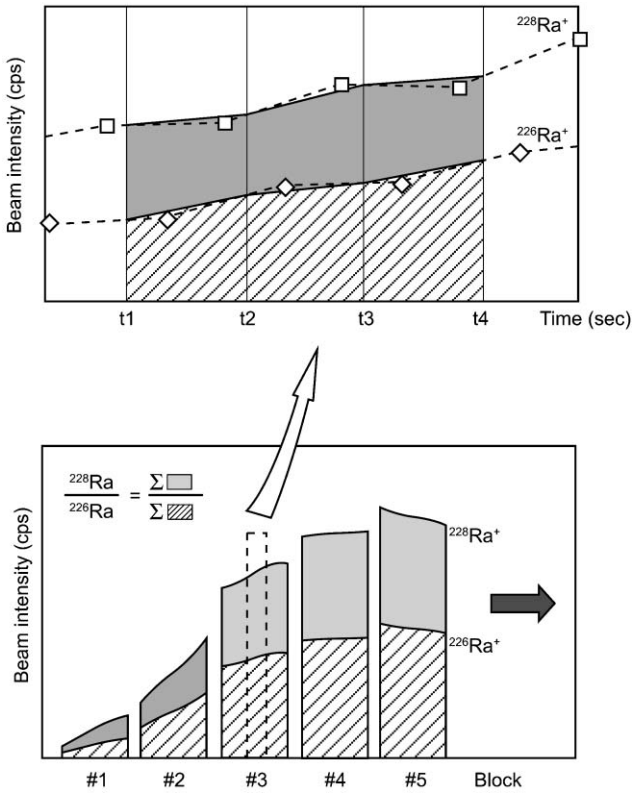

Fig. 2 Calculation of the $^{228}Ra/^{226}Ra$ ratio by TE-TIMS with time-drift correction.

Elution profiles of Sr resin and TRU resin were separately examined by using the MES solution, and the results are shown in Fig. 4. As is suggested by Chabaux *et al.*,[9] who first reported the Ra–Ba separation technique with Sr resin, it seems that the elimination of Ba was easily achieved by using Sr resin with 2.1 mL elution of 3 M HNO_3 while collecting >99% of Ra (Fig. 4a). However, the separation of Ra from REE was clearly insufficient. We therefore used TRU resin to remove L–M REE that could not be separated from Ra in previous steps. As is shown in Fig. 4b, the behavior of REE on TRU resin was individually different; this is probably due to different partition coefficients depending on ionic radii. The separation of Ra from L–M REE (La–Tb) was achieved when total eluant volume was less than 4 mL.

It is worth noting that column procedures utilizing Sr resin and TRU resin used only a 3 M HNO_3 medium, implying that simultaneous separation with a tandem column technique is most efficient. The tandem column separation was tested by using the MES solution. Prior to the tandem arrangement, 0.3 mL of the MES solution was loaded only on Sr resin. After rinsing the resin with 0.4 mL of 3 M HNO_3, the Sr resin column was placed above the TRU resin column. 1.4 mL of 3 M HNO_3 was eluted from the upper column. The Sr resin column was then removed from the top, followed by the addition of 1.5 mL of the eluant to TRU resin. Fig. 4c is the result of the tandem column procedure, showing successful isolation of Ra from the lighter REE (La–Tb).

In Sr resin operation, we found a very small breakthrough of Ba in the Ra fraction (the inset of Fig. 4a). This was not reported by Chabaux *et al.*[9] nor in any research that followed Chabaux's method. Detectable Ba breakthrough started from 1.2 mL of eluant, and it reached 0.02% of relative abundance until 2.1 mL of eluant. Since the Ba abundance in natural silicate rocks generally ranges between 100–500 μg g^{-1}, the amount of Ba present in the Ra fraction corresponds to 2–50 ng when 0.1–0.5 g of sample is used, resulting in serious interference with Ra ionization (see section 3.6). Therefore, the Ra fraction was further purified through newly prepared Sr resin (0.3 mL). By use of this additional step, the amount of Ba remaining in the Ra fraction was reduced to below the detection limit of ICP-MS (<100 pg).

One serious problem of column chemistry using extraction chromatographic resins is the contamination of solutions by organic matter derived from resin that interferes with TIMS analyses, as previously pointed out by Yokoyama *et al.*[14] Therefore, we equipped 0.1 mL of CG-71C at the bottom of the final Sr spec. Although organic matter was drastically decreased compared with that without CG-71C, tiny black pieces of material were still found when the final Ra fraction was dried up. This must have been organic matter that could not be removed completely by CG-71C, including small fragments of the resins used. The black material disappeared when the fraction was repeatedly attacked with the mixture of HNO_3, HF and $HClO_4$. Such an acid treatment did not work well when CG71C was not used, clearly showing that CG-71C was effective in reducing the influx of organic matter from Sr resin into the final fraction.

Recovery yields for the entire separation procedure described above ranged from 83% to 91% (87% on average; $n = 6$) when ~0.5 g of basalt (Miyakejima) were examined.

3.2. Preparation of ^{228}Ra enriched spike

We prepared two ^{228}Ra-enriched spike solutions extracted from $ThCl_4 \cdot 8H_2O$ powder. Approximately 2 g of $ThCl_4 \cdot 8H_2O$

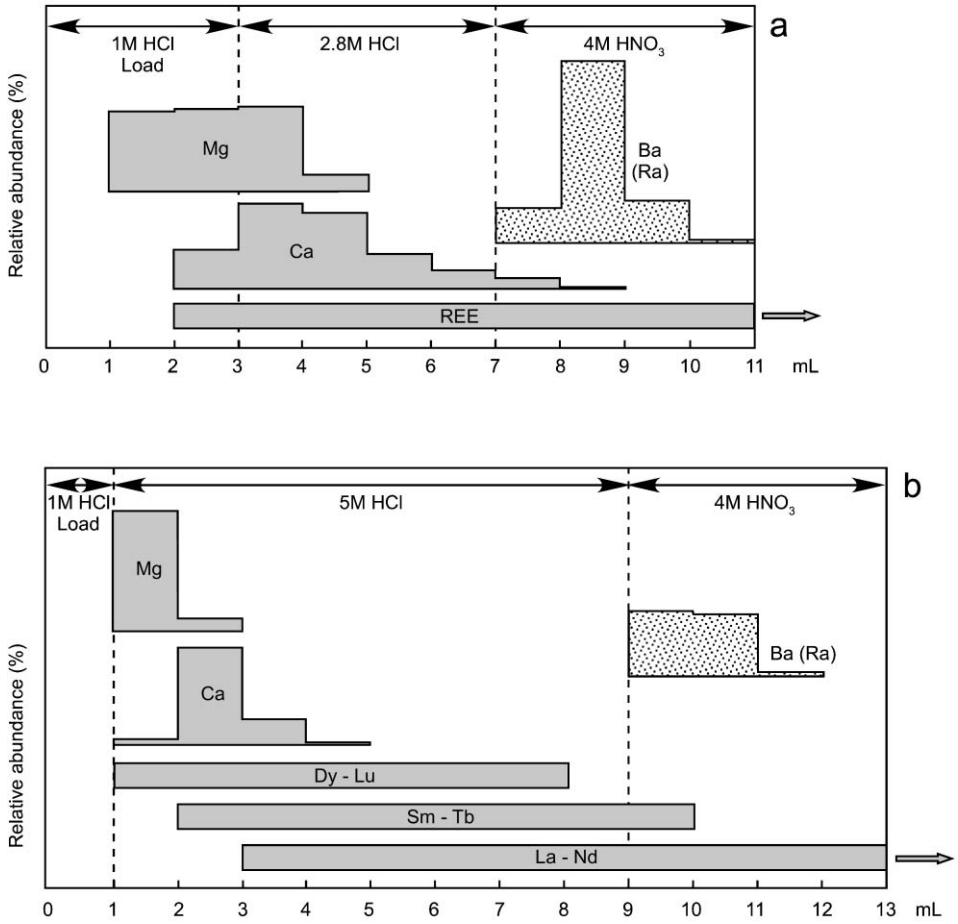

Fig. 3 Elution profiles of 1st column, a, and 2nd column, b, by "mixed-resin". Light–middle REE (La–Tb) and Ba still remain in Ra fraction after these two steps.

was dissolved into 20 mL of 8 M HNO_3. Ra and Th were separately extracted from this solution by passing the solution through 20 mL of anion exchange resin (AG1X8, 200–400 mesh, Muromac). The Ra fraction was further purified by 1 mL of AG1X8 and 0.3 mL of "mixed-resin", and finally purified by the step 5 procedure described in section 2.4.2. Due to the ageing effect of $ThCl_4 \cdot 8H_2O$ over 30 years, ^{228}Ra had radioactively equilibrated with ^{232}Th while ^{226}Ra continued to grow as time elapsed. For this reason, the $^{228}Ra/^{226}Ra$ ratio of the separated Ra was a comparatively low (1.1221 ± 0.0006, $2\sigma_{mean}$, $n = 74$: corrected to July 1st 2003 value). We named this separated solution "Spike-1", and calibrated the concentration by the Ra standard solution (NIST SRM4966). Following preparation of Spike-1, Ra was extracted from the Th fraction (which had been stored over 1 month) using the same separation procedure described above. The $^{228}Ra/^{226}Ra$ ratio of this solution, named "Spike-2", was higher than that of Spike-1 (5.449 ± 0.005, $2\sigma_{mean}$, $n = 13$: corrected to July 1st 2003 value), due to the higher ingrowth rate of ^{228}Ra compared with ^{226}Ra in the very short period of spike ageing, which prevented radioactive equilibrium of ^{228}Ra with respect to ^{232}Th. The concentration of Spike-2 was also determined using the NIST SRM4966 standard solution.

3.3. Performance of total evaporation TIMS

We evaluated the performance of total evaporation Ra isotope analysis with TIMS by repeated measurement of Spike-1 ($^{228}Ra/^{226}Ra$ ratio of ~ 1.1). Sample size was varied from 170 fg to 2 fg, corresponding to ^{226}Ra concentrations of 80 fg to 1 fg. Typical profiles of Ra^+ ion signal intensity and filament temperature are shown in Fig. 5 as a function of time, together with the observed $^{228}Ra/^{226}Ra$ ratio and the change in the integrated $^{228}Ra/^{226}Ra$ ratio. Because of the relatively low Ra^+ intensity, the observed $^{228}Ra/^{226}Ra$ ratio scatters from 1.09 to 1.13 when acquisition time is <500 s. Ra^+ intensity increases as filament temperature increases, and the observed $^{228}Ra/^{226}Ra$ ratio increased by $\sim 1\%$ (from ~ 1.115 to ~ 1.125), clearly indicating mass fractionation during analysis. After 2000 s of acquisition time, the integrated $^{228}Ra/^{226}Ra$ ratio becomes nearly constant as $\sim 90\%$ of the total Ra has been acquired by this point.

The results of repeated Spike-1 analyses are summarized in Table 1. Since ^{228}Ra has a much shorter half-life than ^{226}Ra, all $^{228}Ra/^{226}Ra$ ratios obtained were time-corrected to the values at AM 0:00 of July 1st, 2003. Reproducibility of the $^{228}Ra/^{226}Ra$ ratio increases from 0.20% to 0.91% as the Ra amount decreases from 170 fg to 2 fg. Importantly, the mean value of the $^{228}Ra/^{226}Ra$ ratio for each sample size is constant when analytical reproducibility is taken into account, indicating that any interference that would cause a change in mean values (*e.g.*, mass fractionation, background noise, and blank from filament and activator) is not involved or properly corrected by our method. These results cannot be easily compared to previous studies[4–6,9] because; (1) Spike-1 is our in-house standard and has not been measured elsewhere, and (2) the number of repeated analyses for Ra standard samples reported previously is insufficient ($n = 3$–5) to statistically assess the reproducibility of their technique. However, the reproducibility of our TE-TIMS is expected to be ~ 3 times

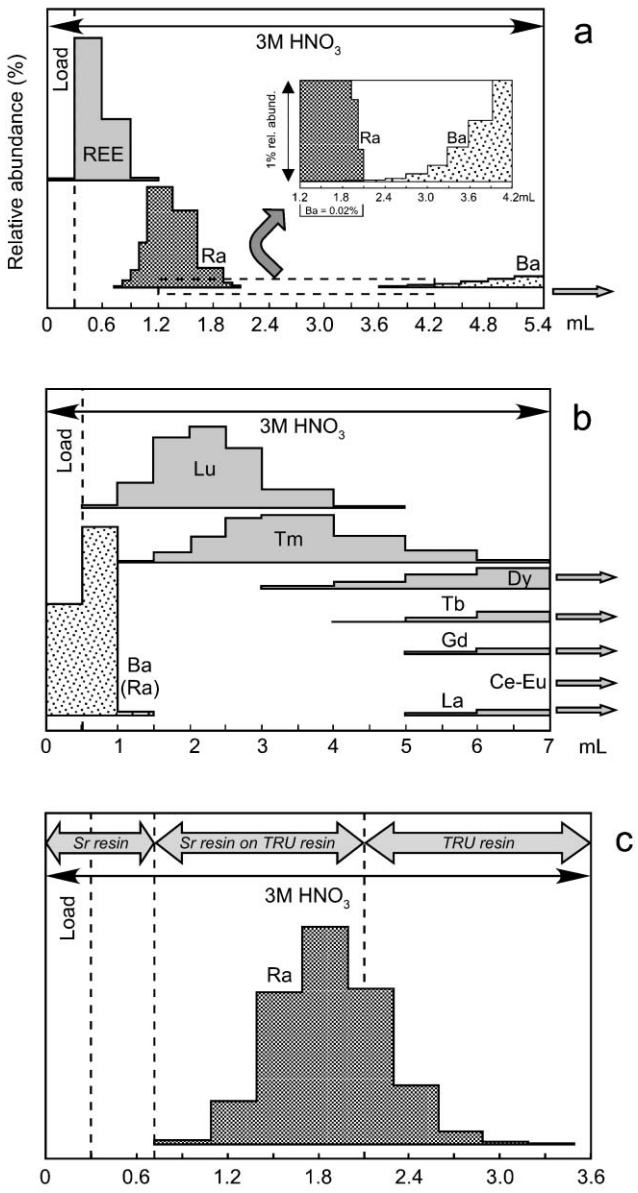

Fig. 4 Elution profiles of Sr resin, a,and TRU resin, b. By combining these resins as a tandem column configuration (see Fig. 1), Ra was separated from light–middle REE (La–Tb) and Ba that could not be removed by the 1st and 2nd column, c. However, breakthrough of a small amount of Ba (0.02%) is observed in the Ra fraction which should be further removed to obtain stable Ra ionization by TIMS. See the text for details.

better than that of a conventional non-TE procedure when we consider the result of our Spike-1 analyses (170 fg, $n = 30$) that was obtained by the procedure following Chabaux *et al.*[9] (Table 1).

For general isotope analysis of elements such as Sr and Nd, analytical precision of an individual run can be calculated as a grand mean of isotope ratios from each scan (typically 100–200 ratios). In the case of total evaporation analysis, however, the isotope ratio is simply calculated from the total signal area of each isotope. We thus evaluated the single run precision of $^{228}Ra/^{226}Ra$ measurement by counting statistics theory as follows:

$$\text{Precision}(2\sigma\%) = 2\cdot\sqrt{\left(\sqrt{N_{\text{eff}}^{228}}\Big/N_{\text{eff}}^{228}\right)^2+\left(\sqrt{N_{\text{eff}}^{226}}\Big/N_{\text{eff}}^{226}\right)^2}\cdot 100 \quad (1)$$

where N_{eff}^{228} and N_{eff}^{226} are the effective number of counts for ^{228}Ra and ^{226}Ra signals that are actually detected by the SEM. Note that N_{eff}^{228} and N_{eff}^{226} are different from ^{228}Ra and ^{226}Ra signal areas used for the calculation of $^{228}Ra/^{226}Ra$ ratio as is shown in Fig. 2 because Ra signals are detected by the mass-jumping method. Fig. 6 shows the $^{228}Ra/^{226}Ra$ ratio of Spike-1 analyses as a function of N_{eff}^{226}. Bold curves in this figure represent theoretical values of single run precision (2σ) that are calculated by eqn. (1). Importantly, most of the $^{228}Ra/^{226}Ra$ data (69 out of 74) are plotted within the theoretical precision curves, suggesting that reproducibility of $^{228}Ra/^{226}Ra$ analysis by TE-TIMS is comparable with the theoretical single run precision. This means that analytical error of $^{228}Ra/^{226}Ra$ ratio in the practical measurement of natural samples can be estimated by eqn. (1), even if the amount of Ra loaded on the filament is unknown. Actual reproducibility of the Spike-1 analysis is 0.15%, 0.27%, and 0.66% (2σ) when N_{eff}^{226} is $>2 \times 10^6$ counts, 5×10^5–2×10^6 counts, and $1 \times 10^5 \sim 5 \times 10^6$ counts, respectively.

3.4. Reproducibility and accuracy of ^{226}Ra determination for natural samples

In order to evaluate the reproducibility and accuracy of our technique for natural silicate rock samples, we determined ^{226}Ra abundance in two GSJ (Geological Survey of Japan) standard rock powders, JB-2 and JR-2. JB-2 is a tholeiitic basalt (SiO_2 = 53.25 wt.%) from Izu-Oshima, Japan, which erupted in 1950 AD. JR-2 is a rhyolitic obsidian (SiO_2 = 75.69 wt.%) from Wada-toge, Japan, which is considered to be old enough for ^{230}Th–^{226}Ra and ^{232}Th–^{228}Ra equilibria (K–Ar age = $\sim$1 Ma).[19] The concentrations of major and trace elements for these standards are given in Imai *et al.*[20] The standard powders were further pulverized using an alumina ceramic swing mill for homogenization. Before sample decomposition, Spike-1 was added for isotope dilution. For JB-2, determination with Spike-2 was also tested by decreasing sample size.

Analytical results are summarized in Table 2. $^{228}Ra/^{226}Ra$ ratios of these samples were not directly measured but calculated using their Th data, as described in Appendix A. Blank corrections were made for all cases (0.03 fg of ^{226}Ra blank per analysis: see section 3.7.1). The reproducibility of JR-2 (2σ = $\sim$0.31%) was at least 2–3 times better than those of previously published conventional TIMS methods for samples with higher Ra abundance (^{226}Ra > 1000 fg g^{-1}),[5,6,9] and comparable to that of MC-ICP-MS (2σ = 0.32% for TML: ^{226}Ra = 3600 fg g^{-1}).[4] In the case of JB-2, it should be noted that, compared with larger size analysis with Spike-1, smaller size analysis with Spike-2 not only showed good agreement for ^{226}Ra abundance, but also had similar reproducibility. This is due to higher enrichment of ^{228}Ra in Spike-2 than Spike-1 (see Appendix B in detail). In previous TIMS studies, the analytical reproducibility of ^{226}Ra determination generally reached 1$\sim$2% (2σ) for samples with lower Ra concentration ($<$100 fg g^{-1}; *e.g.*, MORB), which is 2–4 times worse than our JB-2 results. Therefore, our method must be very effective for the determination of very small quantities of Ra. Furthermore, our method is highly accurate because the ($^{226}Ra/^{230}Th$) ratio of JR-2 displayed secular equilibrium within 0.9% of analytical uncertainty.

3.5. Measurement of the $^{226}Ra/^{228}Ra$ ratio in natural samples

The $^{226}Ra/^{228}Ra$ ratio in natural samples was determined for two silicate rocks, JR-2 and CA076. CA076 is a Mt. Cameroon alkali basalt, erupted in 1999 AD, of which SiO_2 = 46.2 wt.% (F.T. Aka, personal communication). As is shown in Table 3, the reproducibility of $^{226}Ra/^{228}Ra$ analysis was 1.0% for JR-2 and 0.35% for CA076, and they are comparable or coincidently better than their precisions of individual runs which were estimated by eqn. (1).

The ($^{228}Ra/^{232}Th$) ratio of JR-2 was equal to unity within analytical uncertainty, clearly supporting the accuracy of our

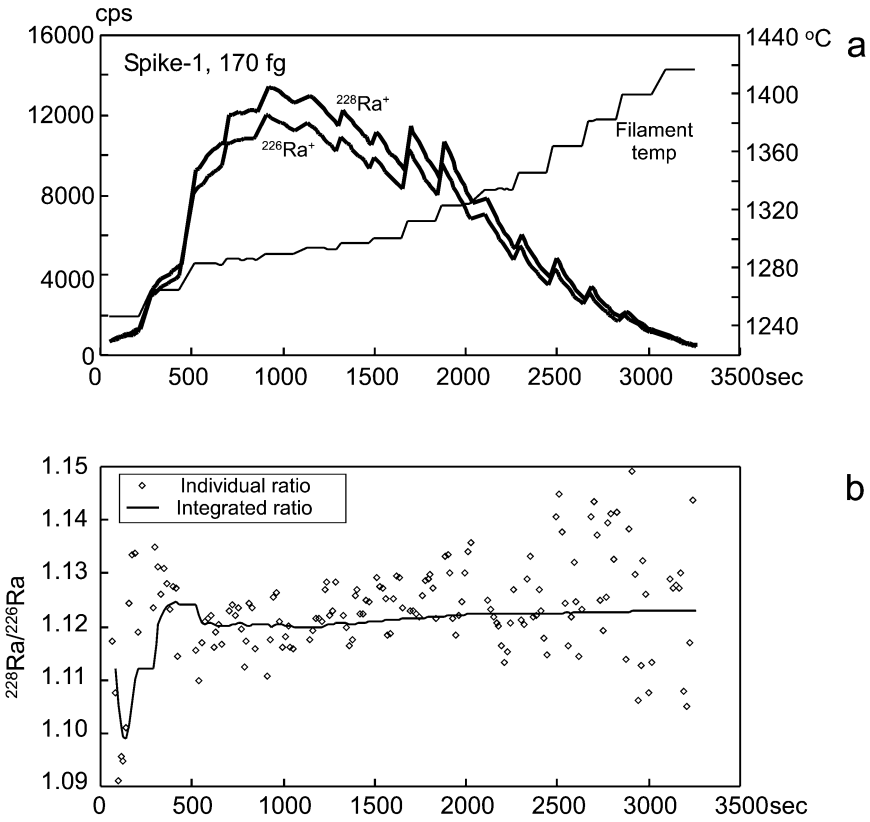

Fig. 5 a, Ra^+ ion beam profiles and the change of filament temperature during TE-TIMS analysis for Spike-1 (170 fg) as a function of time. b, The variation of individual $^{228}Ra/^{226}Ra$ ratio and integrated ratio which is calculated as shown in Fig. 2. All ratios are time-corrected to July 1st, 2003, values.

Table 1 Summary of Spike-1 analysis

Ra/fg	$^{228}Ra/^{226}Ra$	Ra $\pm$ 2σ	2σ (%)	*n*
170	1.1220	$\pm$0.0023	0.20	22
85	1.1229	$\pm$0.0023	0.21	12
40	1.1224	$\pm$0.0040	0.35	7
16	1.1228	$\pm$0.0038	0.34	5
8	1.1235	$\pm$0.0049	0.44	8
4	1.1210	$\pm$0.0051	0.46	11
2	1.1207	$\pm$0.0102	0.91	9
All	1.1221	$\pm$0.0006[b]	0.05	74
170	*1.1231*	*$\pm$0.0079*	*0.70*	*30*

[a] Time correction at AM 0:00 July 1st 2003 was done for all data. [b] 2σ mean value. [c] Italic: not TE-TIMS.

isotope analysis of Ra. In contrast, sample CA076, in which only 4 years had elapsed between eruption and Ra analysis, also showed ^{232}Th–^{228}Ra equilibrium within error limits, whereas the sample was in ^{230}Th–^{226}Ra disequilibrium (see the footnote of Table 3). This implies that the last Ra–Th fractionation of the parental magma for CA076 took place >30 yr and <8000 yr before the present.

3.6. Detection sensitivity of Ra

The detection sensitivity of our method can be calculated by comparing the area of the total Ra signal and the amount of Ra

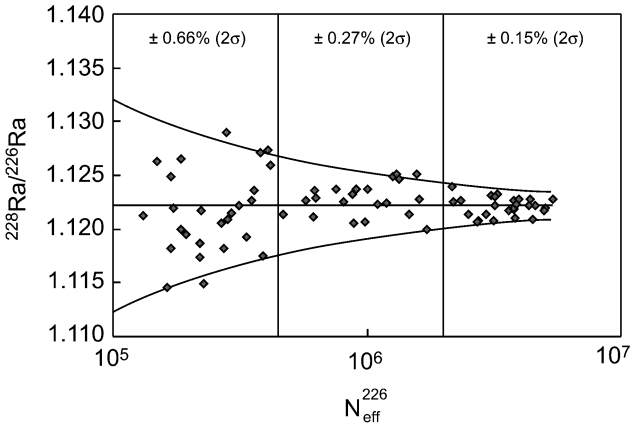

Fig. 6 Relationship between determined $^{228}Ra/^{226}Ra$ ratios of Spike-1 (170–2 fg) and total number of $^{226}Ra^+$ ions actually counted by the SEM. The curves are theoretical values of single run precision calculated by eqn. (1), based on counting statistics law. $^{228}Ra/^{226}Ra$ ratios are time-corrected to July 1st, 2003, values.

actually loaded. In Ra isotope analyses of Spike-1 (section 3.3.3), the detection sensitivity ranged from 5% to 20% (average 10%). This is comparable with that of a previous TIMS study (10–15% for pure standard), and 10–40 times better than MC-ICP-MS analysis.[4,5] Judging from the lower detection sensitivity of MC-ICP-MS and counting statistics law, we infer that

Table 2 Repeated analysis of Ra abundance in GSJ standards by TE-TIMS

Sample	Matrix/mg	Ra used/fg	^{226}Ra conc./fg g^{-1}	2σ (%)	*n*	Ra spike	Th/μg g^{-1}	($^{230}Th/^{232}Th$)	($^{226}Ra/^{230}Th$)[b]
JR-2[a]	50–80	185–300	3696 $\pm$ 12	0.31	5	Spike-1	31.57	1.055	0.998 $\pm$ 0.009
JB-2	330	27	81.13 $\pm$ 0.49	0.61	5	Spike-1	0.269	1.205	2.253 $\pm$ 0.024
JB-2	75	6	81.25 $\pm$ 0.51	0.63	5	Spike-2	0.269	1.205	2.257 $\pm$ 0.024

[a] Th data of JR-2 is after Yokoyama et al.[22], and that for JB-2 is analyzed by T. Yokoyama (unpublished). [b] Error includes uncertainty of Th analysis.

Table 3 Repeated analysis of $^{226}Ra/^{228}$ Ra ratio in natural samples

Sample	Age	Matrix/mg	Ra used/fg	^{228}Ra used/fg	$^{226}Ra/^{228}Ra$	2σ (%)	In-run precision (%)	n	($^{228}Ra/^{232}Th$)
JR-2	1 Ma	300	1000	3.8	293.1 ± 2.9	1.0	0.6–0.9	5	0.999 ± 0.014
CA076[a]	1999 AD	500	500	1.7	316.4 ± 1.1	0.35	1.1–1.5	4	0.998 ± 0.012

[a] Th = 8.31 μg gl^{-1} ($^{230}Th/^{232}Th$) = 0.982, and ($^{226}Ra/^{230}Th$) = 1.164, analyzed by T. Yokoyama (unpublished data).

the good reproducibility of ^{226}Ra determination by MC-ICP-MS reported by Pietruszka *et al.*[4] (0.32% for TML, n = 5; 0.09% for Kil1919, n = 3) might be a coincidence due to the small number of analyses. The large variation in the detection sensitivity for Spike-1 observed in this study probably resulted from differences arising from loading conditions, because relatively lower detection sensitivity was associated with instances where the sample area loaded on the filament was slightly larger (*ca.* 2 mm × 2 mm square) than that with the standard spot-loading technique (*ca.* 1 mm × 1 mm square).

In the case of natural samples, Cohen and O'Nions[5] reported that the detection sensitivity of Ra decreased than that of pure standard owing to the presence of an impurity that could not be separated by column chemistry. We found that this is due to the interference of Ba if it remains as an impurity in the separated Ra fraction, which was also pointed out by Volpe *et al.*[6] Fig. 7 shows profiles of Ra^+ ion beam intensity and filament temperature during analyses of JB-2 (matrix = 300 mg) by TE-TIMS. Fig. 7a is the case for which final Ra purification procedure (Step 5 of section 2.4.2) was skipped. Ba abundance in the Ra fraction was determined to be 16 ng by ICP-MS, corresponding to 0.02% of the initial Ba (68.7 μg). This matches well with the degree of Ba breakthrough observed in the elution test of Sr resin (Fig. 4a). In this case, the Ra^+ ion signal increased very slowly until the filament temperature of 1450 °C, then the signal suddenly increased at 1500 °C, followed by rapid decrease in the next 200 s (Fig. 7a). The filament temperature to obtain the most intense Ra^+ signal was approximately 200 °C higher than that of Spike-1 analysis (Fig. 5). This clearly indicates that Ra ionization was significantly suppressed by the existence of Ba, resulting in the lower detection sensitivity for natural samples than pure standard.

In contrast, Fig. 7b is the result after complete chemical separation, including Step 5, has been carried out. It was confirmed by ICP-MS that the final Ra fraction contained a Ba abundance lower than the detection limit (<100 pg). The beam profile is similar to that for Spike-1 (Fig. 5), and the detection sensitivity was calculated to be 7% by assuming a 90% recovery yield of Ra for the whole chemical procedure. For the other natural samples in which Ra was separated by the same procedure, the detection sensitivity ranged from 5% to 10% (rarely up to 15%), which is comparable to the case of Spike-1 analyses. This clearly indicates that our separation method is very effective in isolating Ra from natural samples pure enough for the precise analysis of the Ra isotope with TIMS.

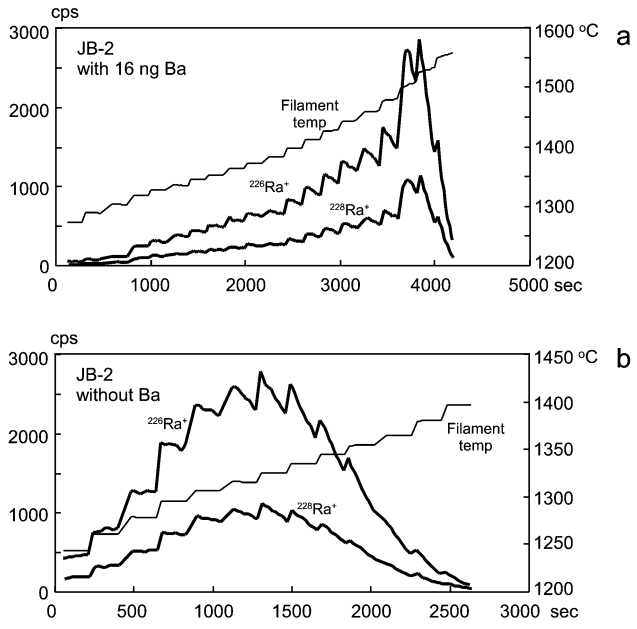

Fig. 7 Ra^+ ion beam profiles and the change of filament temperature during TE-TIMS analysis for JB-2 containing 16 ng of Ba, a, and <100 pg of Ba, b.

3.7. Blanks of our method

3.7.1. Total procedural blanks for Ra. The total procedural ^{226}Ra blank of our method, including sample decomposition, column chemistry, and Ra loading on the filament, was measured four times by using Spike-2. The amount of acids used is equal to that for 0.5 g of sample digestion. All blank tests showed values lower than the detection limit (3σ uncertainty of Spike-2: 0.02 fg) except for one run (0.05 fg). Therefore, we can expect typical total procedural blank values for ^{226}Ra analysis to be ~0.03 fg by averaging the four blank runs. This implies that at least 3 fg of ^{226}Ra is required if one would like to suppress the effect of the blank to <1%.

3.7.2. Background noise of the detector. Fig. 8a shows fluctuation in the background noise of the SEM over a long period (May 31–August 19, 2003) that was measured as a grand mean of 110 scans (16 s integration per one scan) for each

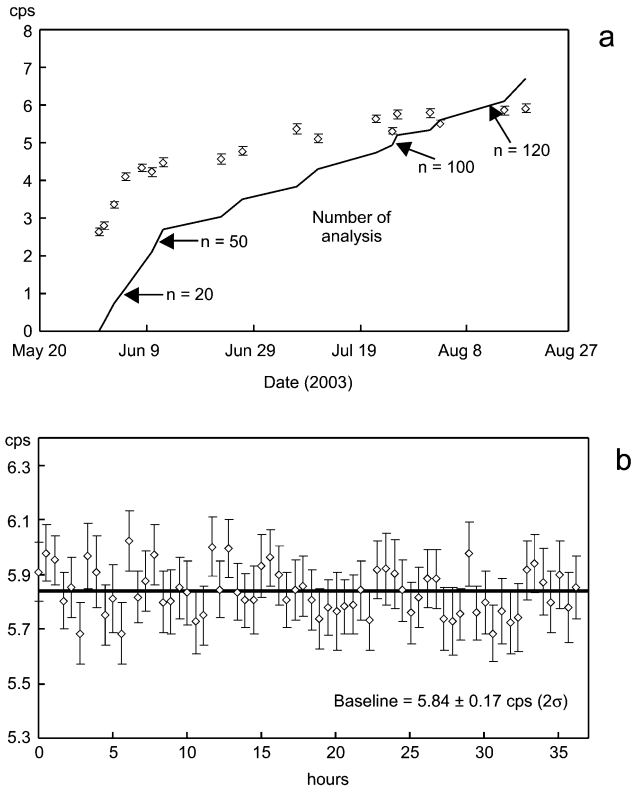

Fig. 8 Fluctuation of background noise of the detector for long period, a, and a short period, b. No Ra analysis was carried out during the background measurement for the short period.

Table 4 Effect of baseline error to observed Ra isotope data

Sample	Ra/fg	Original data		Baseline +0.2 cps	
		$^{228}Ra/^{226}Ra$	2σ%	$^{228}Ra/^{226}Ra$	Diff.%
Spike-1	170	1.1227 ± 0.0015	0.13	1.1227	0.0004
Spike-1	85	1.1213 ± 0.0017	0.15	1.1213	0.0004
Spike-1	40	1.1222 ± 0.0029	0.26	1.1222	0.001
Spike-1	16	1.1213 ± 0.0045	0.40	1.1213	0.003
Spike-1	8	1.1214 ± 0.0057	0.51	1.1214	0.004
Spike-1	4	1.1213 ± 0.0085	0.76	1.1214	0.01
Spike-1	2	1.1217 ± 0.0101	0.90	1.1220	0.03
		$^{226}Ra/^{228}Ra$	2σ%	$^{226}Ra/^{228}Ra$	Diff.%
JR-2	1000	292.6 ± 1.8	0.63	292.9	0.10
JR-2	1000	293.3 ± 2.0	0.70	294.0	0.23

analysis. Prior to our initial analyses of Ra isotopes (February 2002), the noise value of the SEM was essentially negligible at <0.03 cps, but drastically increased to a few cps after 1 year's usage. Another SEM of this TIMS that is not used for Ra isotope analysis showed no increase of background noise from <0.03 cps during the same period. As is shown in Fig. 8a, the increase of the SEM background noise strongly correlates with the total number of Ra isotope analyses during this period. Therefore, we inferred that the increase of the SEM background noise must be due to the *in-situ* radioactive decay of ^{228}Ra that was adsorbed on the first dynode of the SEM.

Fig. 8b shows fluctuation of the SEM background noise for a short period (36 h, August 11–12, 2003). During this period, no Ra isotope analysis was performed, and the baseline was constant to within ± 0.2 cps fluctuation when analytical errors are taken into account. As is shown in Table 4, 0.2 cps uncertainty of the SEM background noise does not affect the $^{228}Ra/^{226}Ra$ ratio obtained, even in the case of small sample sizes (2 fg of Spike-1) or, in the case of a non-spiked run, for JR-2. The increase of the SEM background noise was 3.3 cps after 120 sample analyses (Fig. 8a), corresponding to 0.03 cps sample^{-1}. We thus measured the SEM background noise after every 5 samples, and subtracted the obtained value from acquired Ra data.

3.7.3. Mass interferences from activator and filament. Mass interferences on $m/z = 226$ and 228 that derived from Ta oxide solution and the W filament were checked by loading 1 μL of Ta oxide solution onto a W filament without any sample, and then analyzed with data acquisition procedures identical to those of actual analytical conditions ($m/z = 226$ and 228, 1250 °C–1400 °C). To avoid the SEM background noise (see above), the interferences were detected by a SEM with RPQ system that had not contaminated by ^{228}Ra. Observed mass interferences were less than the dark-noise of the RPQ-SEM detector (<0.03 cps) for both $m/z = 226$ and 228, implying that mass interferences from the activator and filament are negligible.

4. Concluding remarks

We have established a new method for precise and accurate determination of Ra abundance and isotope ratio in natural samples by employing a TE-TIMS technique together with a new separation procedure for Ra utilizing sequential chromatographic separation. The reproducibility of Spike-1, which has $^{228}Ra/^{226}Ra$ of ~1.1, was a function of sample loaded, ranging from 0.2%–0.9% (2σ) for 170 to 2 fg of Ra usage. The in-run precision of Ra isotope analysis of our method can be estimated from counting statistics law. Determination of ^{226}Ra abundance and $^{226}Ra/^{228}Ra$ ratio in silicate rock samples was possible with 0.3–0.6% and 1–1.5% of analytical uncertainties (2σ), respectively. This is 2–3 times better than previously published conventional TIMS procedures. The accuracy of our method was confirmed by measuring ($^{226}Ra/^{230}Th$) and ($^{228}Ra/^{232}Th$) ratios in a 1 Myr-aged geological sample. The analytical improvements, suggested in this paper, will improve the quality of Ra analyses. High precision Ra analyses have a wide range of application but are especially important in geochronological studies, such as the evaluation of timescales for mineral crystallization in magma chambers that use a (^{226}Ra)/Ba–(^{230}Th)/Ba isochron diagram (summarized in Condomines *et al.*[21]). Precise determination of ^{226}Ra to better than 1% analytical error will make it possible to distinguish small differences in the crystallization time of different minerals in a magma chamber.

One of the disadvantages of our method arises from the mass-jumping analysis mode of TIMS. The loss of $^{226}Ra^+$ or $^{228}Ra^+$ signals during the acquisition of the other mass would cause not only the deterioration of the precision of $^{228}Ra/^{226}Ra$ ratio due to the decrease of total number of counts, but also mis-counting of signals when instantaneous signal change occurs. A new generation TIMS, Triton TI (Finnigan) enables simultaneous accumulation of $^{226}Ra^+$ and $^{228}Ra^+$ ion signals with multi-SEM configuration. Although precise conversion factor between two SEMs comparable to or even smaller than the precision of $^{228}Ra/^{226}Ra$ ratio is required, total evaporation Ra analysis using TIMS equipped with multi-SEM would improve the precision of Ra isotope analysis better than that reported in this study.

Acknowledgements

We thank A. Makishima and all the members of PML for their analytical support and useful discussion. Y. Miyata is acknowledged for his useful advice on total evaporation TIMS. We are grateful to R. King and I. Campbell for improving this paper. We thank F. T. Aka for providing the sample from Mt. Cameroon. This research was supported by the Japanese Society for the Promotion of Science (JSPS) fellowships for Japanese Junior Scientists to T.Y., Grants-in-Aid for Scientific Research from the Ministry of Education, Culture, Sports, Science and Technology, Japan (Monbu-Kagaku-sho) to E.N., and "Center of Excellence in the 21st Century in Japan" (E.N.).

Appendix

A. Calculation of ^{226}Ra abundance

For the determination of ^{226}Ra abundance in natural samples by isotope dilution, the $^{228}Ra/^{226}Ra$ ratio of the sample prior to spike addition is required. However, if one can assume ^{232}Th–^{228}Ra radioactive equilibrium in the sample (for cases where at least 30 years have elapsed since the last Th–Ra fractionation), the amount of ^{228}Ra in the sample may be calculated from that of ^{232}Th as follows:

$$C_{228} = C_{232} \cdot \frac{\lambda_{232}}{\lambda_{228}} \cdot \frac{228}{232} \quad \text{(A1)}$$

where C is the concentration in the sample, λ is the decay constant, and subscripts 228 and 232 represent ^{228}Ra and ^{232}Th. C_{228} is also expressed as follows:

$$C_{228} = C_{Ra} \cdot \frac{228 \cdot R_n}{226 + 228 \cdot R_n} \quad \text{(A2)}$$

where C_{Ra} is the total Ra concentration in the sample, and R_n is $^{228}Ra/^{226}Ra$ ratio of the sample. For isotope dilution, C_{Ra} is given by

$$C_{Ra} = C_{sp} \cdot \frac{R_{sp} - R_m}{R_m - R_n} \cdot \frac{226 + 228 \cdot R_n}{226 + 228 \cdot R_{sp}} \cdot \frac{W_{sp}}{W_n} \quad \text{(A3)}$$

where C_{sp} is the Ra concentration of the spike, R_{sp} and R_m are

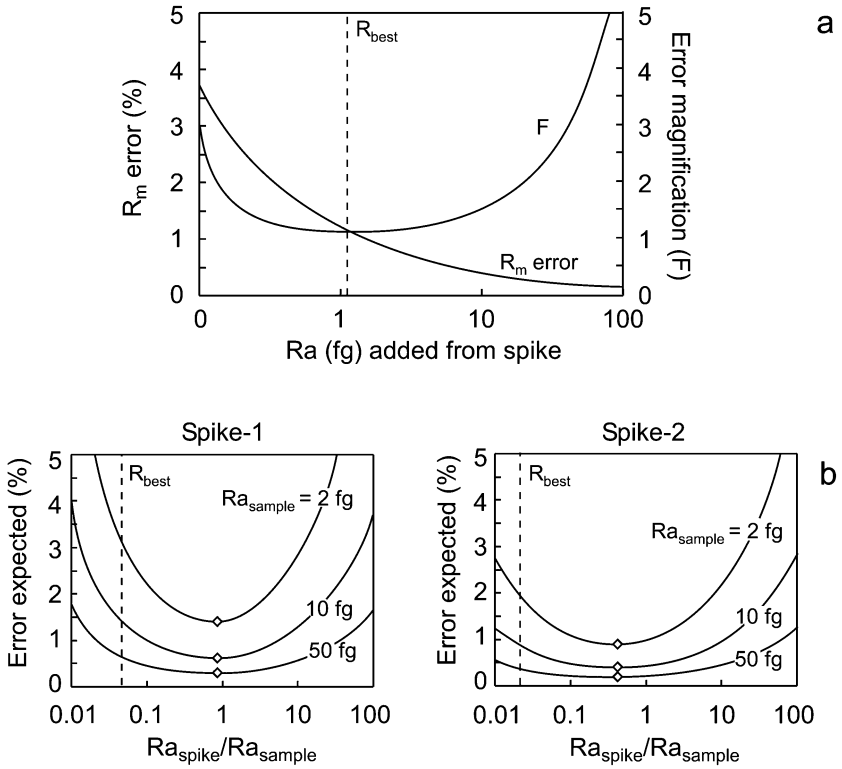

Fig. 9 a, Error magnification factor (F) calculated from equation (B2) and the error of R_m calculated by equation (1), as a function of Ra amount

the $^{228}Ra/^{226}Ra$ ratios of the spike and spike/sample mixture, and W_{sp} and W_n are weighed amounts of the spike and the sample. By eliminating C_{228} and R_n from these equations, C_{Ra} is given by

$$C_{Ra} = C_{232}\cdot\frac{\lambda_{232}}{\lambda_{228}}\cdot\frac{228}{232}\cdot\left(1+\frac{226}{228\cdot R_m}\right) + C_{sp}\cdot\frac{R_{sp}-R_m}{226+228\cdot R_{sp}}\cdot\frac{226}{R_m}\cdot\frac{W_{sp}}{W_n} \quad (A4)$$

Once C_{Ra} has been obtained, R_n is calculated by using equations (A1) and (A2). The ^{226}Ra concentration in the sample (C_{226}) is finally obtained by substituting C_{Ra} and R_n into the following equation:

$$C_{226} = C_{Ra}\cdot\frac{226}{226+228\cdot R_n} \quad (A5)$$

Because Th concentration in the sample is usually determined in the study of U-series disequilibria for natural samples, only a spiked run is needed for the determination of Ra when ^{232}Th–^{228}Ra radioactive equilibrium can be assumed.

B. Ideal mixing ratio of spike and sample

In isotope dilution, error from isotope analysis propagates on the result of abundance determination as a function of spike/sample mixture ratio, and the error magnification factor (F) is given by

$$F = \frac{(R_{sp}-R_n)\cdot R_m}{(R_m-R_n)\cdot(R_{sp}-R_m)} \quad (B1)$$

where R_n, R_{sp} and R_m are isotope ratios of the sample, the spike, and spike/sample mixture. The best spike/sample mixing ratio (R_{best}) to minimize F is given by

$$R_{best} = \sqrt{R_n\cdot R_{sp}} \quad (B2)$$

The change of F is shown in Fig. 9 as a function of Ra amount added from spike. In the determination of Ra by TE-TIMS, however, equation (B2) does not always give "true" R_{best} because the precision of $^{228}Ra/^{226}Ra$ ratio is strongly controlled by counting statistics of ^{226}Ra and ^{228}Ra ion signals, as is described in section 3.3, depending on how much ^{226}Ra and ^{228}Ra are artificially added from the spike (Fig. 9).

Fig. 9b shows expected analytical errors of ^{226}Ra abundance determination calculated by multiplying the error of R_m and F obtained from equations (1) and (B1), respectively. The sample is supposed to have $^{228}Ra/^{226}Ra = 0.002$, and both Spike-1 ($^{228}Ra/^{226}Ra = 1.1$) and Spike-2 ($^{228}Ra/^{226}Ra = 5.4$) usage are simulated by varying the sample amount from 2 fg to 50 fg. In any case, the amount of spike addition that would give the minimum error on ^{226}Ra abundance determination (diamonds in Fig. 9b) is much higher than that for R_{best} in equation (B1). It is worth noting that Spike-2 is very effective in decreasing the expected analytical error, especially for very small amounts of Ra usage (<10 fg) because its ^{228}Ra enrichment is 5 times higher than that of Spike-1. In contrast, the minimum expected error becomes very small (<0.3%) for both types of spike when the sample amount exceeds 50 fg. Therefore, we separately used Spike-1 and Spike–2 for samples containing larger (>50 fg) and smaller (<50 fg) amount of Ra, respectively.

References

1 M. Ivanovich and R. S. Harmon, *Uranium-series Disequilibrium: Applications to Earth, Marine, and Environmental Sciences*, Oxford University Press, New York, 1992.
2 B. Bourdon, G. M. Henderson, C. C. Lundstrom and S. P. Turner, *Uranium-series Geochemistry*, Geochemical Society, Mineralogical Society of America, Washington, 2003.
3 S. Nakai, S. Fukuda and S. Nakada, *Analyst*, 2001, **126**, 1707–1719.
4 A. J. Pietruszka, R. W. Carlson and E. H. Hauri, *Chem. Geol.*, 2002, **188**, 171–191.
5 A. S. Cohen and R. K. O'Nions, *Anal. Chem.*, 1991, **63**, 2705–2708.
6 A. M. Volpe, J. A. Olivares and M. T. Murrell, *Anal. Chem.*, 1991, **63**, 913–916.

7 A. J. Pietruszka, K. H. Rubin and M. O. Garcia, *Earth Planet. Sci. Lett.*, 2001, **186**, 15–31.
8 R. Fiedler, D. Donohue, G. Grabmueller and A. Kurosawa, *Int. J. Mass Spectrom. Ion Processes*, 1994, **132**, 207–215.
9 F. Chabaux, D. Ben Othman and J. L. Brick, *Chem. Geol.*, 1994, **114**, 191–197.
10 E. P. Horwitz, M. L. Dietz and D. E. Fisher, *Anal. Chem.*, 1991, **63**, 522–525.
11 E. Nakamura, A. Makishima, T. Moriguti, K. Kobayashi, C. Sakaguchi, T. Yokoyama, R. Tanaka, T. Kuritani and H. Takei, *Inst. Space Astronaut. Sci. Rep. SP.*, 2003, **16**, 49–101.
12 A. Makishima and E. Nakamura, *Geostand. Newslett.*, 1997, **21**, 307–319.
13 A. Makishima, K. Kobayashi and E. Nakamura, *Geostand. Newslett.*, 2002, **26**, 41–51.
14 T. Yokoyama, A. Makishima and E. Nakamura, *Chem. Geol.*, 2001, **181**, 1–12.
15 T. Yokoyama, A. Makishima and E. Nakamura, *Anal. Chem.*, 1999, **71**, 135–141.
16 T. Yokoyama, A. Makishima and E. Nakamura, *Chem. Geol.*, 1999, **157**, 175–187.
17 M. Yoshikawa and E. Nakamura, *J. Mineral. Petrol. Econ. Geol.*, 1993, **88**, 548–561.
18 P. A. Gorry, *Anal. Chem.*, 1990, **62**, 570–573.
19 I. Kaneoka and M. Suzuki, *J. Geol. Soc. Jpn*, 1970, **76**, 309–313.
20 N. Imai, S. Terashima, S. Itoh and A. Ando, *Geochem. J.*, 1995, **29**, 91–95.
21 M. Condomines, P.-J. Gauthier and O. Sigmarsson, in *Uranium-series Geochemistry* eds. B. Bourdon, G. M. Henderson, C. C. Lundstrom, and S. P. Turner, Geochemical Society, Mineralogical Society of America, Washington, 2003, pp. 125–174.
22 T. Yokoyama, K. Kobayashi, T. Kuritani and E. Nakamura, *J. Geophys. Res.*, 2003, **108**(No. B7); DOI:10.1029/2002JB002103.